A Ringing Metric to Evaluate the Quality of Images Restored using Iterative Deconvolution Algorithms

M. Balasubramanian
Computer science, LSU.
madhu@csc.lsu.edu

S.S. Iyengar
Computer science, LSU.
iyengar@csc.lsu.edu

J. Reynaud
Eye center, LSUHSC.
jreyna@lsuhsc.edu

R.W. Beuerman
Ophthalmology, LSUHSC.
rbeuer@lsuhsc.edu

Abstract

Iterative deconvolution algorithms exhibit increased ringing artifacts at higher number of iterations. Quantitative image analysis techniques such as optical flow algorithms are sensitive to these artifacts. We propose to use an image quality metric to identify the terminal step of iterative restoration algorithms. Frequency based metrics have difficulties in distinguishing the ringing artifacts from the image features. Spatial analysis techniques require extensive processing making them unsuitable for real-time image quality measurement as needed in iterative image restoration. We propose a novel ringing metric using binary morphological operators and demonstrate the method on the images of random cotton fibers acquired using white light confocal microscope.

1. Introduction

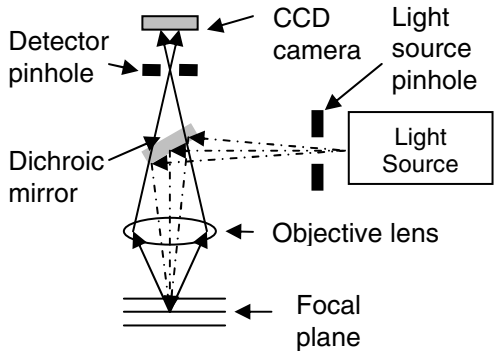

Figure 1. Schematic representation of a confocal microscope.

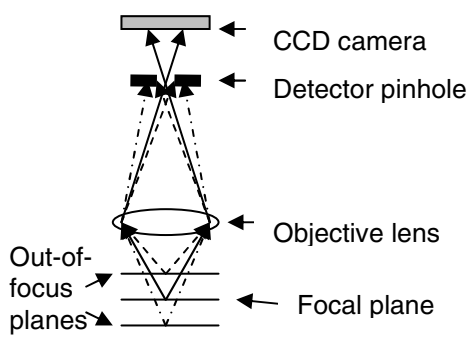

Figure 2. Principle of a pinhole detector.

The basic concept of confocal microscopy was originally developed by Marvin Minsky. A confocal microscope can be used to image a 3D microscopic specimen at various depths without physical sectioning. Figure 1 shows the schematic representation of a confocal microscope. Light from a light source passes through a pinhole, gets reflected by a dichroic mirror and illuminates the specimen. The light reflected from the specimen passes through the dichroic mirror and a series of detector pinholes mounted on a rotating disk and forms an image of the specimen in the CCD camera. The role of the detector pinhole is crucial in allowing only the reflected light from the focal plane. Figure 2 shows the role of a detector pinhole in blocking the light from the out-of-focus planes. The size of the detector pinhole determines the

Proceedings of the 18th International Conference on Systems Engineering (ISCEng'05)
0-7695-2359-5/05 $20.00 © 2005 **IEEE**

amount of light from the out-of-focus planes reaching the CCD camera. Smaller pinhole size results in sharper images, but also limits the amount of light reaching the CCD camera. Thus a compromise must be reached.

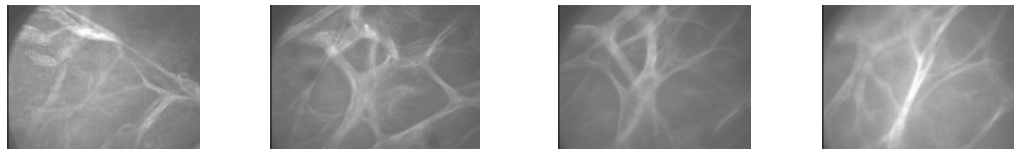

Depth: 0 microns Depth: 80 microns Depth: 160 microns Depth: 240 microns

Figure 3. Image stack of lamina cribrosa of cow retina

Figure 3 shows a stack of images of lamina cribrosa of cow retina. Confocal microscopy is well suited for imaging thick specimens, cells and molecules. A non-laser light source is suitable for imaging *in vivo*. White light sources such as xenon lamps provide a non-coherent laser light source [1, 2]. The images used in this research were obtained using a custom built white light confocal microscope (WLCM) at the LSU Eye Center, New Orleans.

An image obtained from a confocal microscope can be modeled as $g = h * f + n$, where g is the image observed using WLCM, f is the original image at the object plane, * is the convolution operator, h is the point spread function (PSF) of the WLCM and n is the additive noise present in the optical system. Image restoration algorithms compute an estimate of the original image f using the observed image g and the impulse response h of the WLCM [3, 4]. These algorithms can be broadly classified as 1. Direct methods [5], 2. Iterative methods [6] and 3. Blind deconvolution methods [7]. The direct and iterative methods estimate the original image f using the observed image g and the PSF h. The blind deconvolution algorithms estimate both the original image f and the PSF h from the observed image g. The direct methods are faster but the solution computed is sensitive to the image noise [3]. As opposed to the blind deconvolution, iterative deconvolution algorithms use *a priori* knowledge of the blurring process in computing an estimate of the original image f.

Iterative deconvolution algorithms derive an estimate of the original image f from the observed image g in iterative steps. A usual stopping criteria for an iterative deconvolution algorithm is an error functional of the form $\| \bar{f}_{k+1} - \bar{f}_k \|$ where, $\bar{f}_k$ is the estimate of the original image at k^{th} iteration. We observed that the images restored using iterative deconvolution algorithms such as Lucy-Richardson restoration algorithm exhibit prominent oscillations around the edges with sharp intensity transitions at higher number of iterations. These spurious oscillations around the edges are known as ringing artifacts. Thus an error functional based on a difference measure cannot measure the amount of ringing present introduced in the images during restoration. Hence there is a clear need to incorporate an image quality metric, specifically a ringing metric in place of an error functional to identify an appropriate stopping criterion for an iterative deconvolution algorithm.

The objective quality metrics such as peak-signal-to-noise ratio (PSNR) and MSE metrics do not correlate with the quality assessed by a human visual system [8]. The assigned image quality metric should confirm with the human visual perception and hence assigning an objective image quality metric is a very difficult problem [9]. Image quality assessment can be broadly classified as no-reference methods and full-reference methods. The full-reference methods compute a quality metric of a given image using a reference or undistorted-original image. No-reference methods do not require a reference image in assigning a quality metric. Recently several image quality metrics has been proposed to measure the blur and blocking artifacts introduced by image/video compression algorithms [10-13]. A frequency based

ringing metric will have difficulties in differentiating the ringing artifacts from the image features. Spatial analysis techniques require extensive row-by-row processing [11] and are not suitable for real-time image quality measurement as needed in iterative deconvolution algorithms.

We propose a novel ringing metric using simple binary morphological operations to measure the amount of ringing artifacts present in an image. Section 2 explains an experimental procedure to estimate the PSF of a WLCM. Section 3 investigates the choice a contrast based quality metric and the proposed ringing metric. Section 4 presents the results of our proposed method. In section 5 we conclude this research and suggest directions for future work.

2. Restoration of white light confocal microscope images

The impulse response of an imaging system can be obtained by imaging a point light source under the usual imaging conditions. In an ideal imaging system, the intensity distribution of this point light source image will closely resemble a delta function. Due to imperfect imaging conditions and limitations on the pinhole aperture size, the observed single point will instead have a Gaussian signature as shown in figure 3a. Thus the impulse response is referred as the smearing or point spread function (PSF) of the optical system [14].

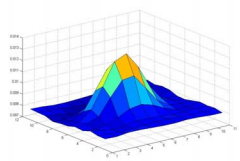

Figure 3a. Intensity plot of PSF

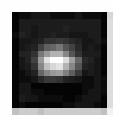

Figure 3b. Image of a 5-micron sphere

We determined the PSF of the WLCM by imaging 5-micron diameter micro-spheres, in focus, under the usual imaging conditions as in [15-18]. We reduce the noise sensitivity of the observed PSF by averaging 3 frames of on-focus micro-spheres. The PSF is then normalized such that its pixel intensities sum to 1.0 to conserve the energy arising from each pixel positions. Now the observed image g can be iteratively restored using Lucy-Richardson (LR) deconvolution algorithm [19] as follows.

$$\bar{f}_{k+1}(x,y) = \bar{f}_k(x,y)\Big(\big(h(-x,-y) * g(x,y) \big) / \big(h(x,y) * \bar{f}_k(x,y) \big) \Big)$$

Section 3 investigates the choice of a contrast measure to assess the quality of the restored images and proposes a ringing metric to measure the ringing artifacts present in the restored images.

3. Image quality metrics

3.1 Contrast measure

Deconvolution is a deblurring process and the restored images typically exhibit sharp edges with an overall increase in the high frequency contents of the image. Therefore, our first choice for an image quality metric was to use a gradient based method. We define a contrast measure using Sobel gradient operators S_x *and* S_y as in [20] as follows.

Gradient at pixel (m, n): $$S(m,n) = \sqrt{\left(G_x(m,n)^2 + G_y(m,n)^2\right)}$$

Focus/Contrast measure: $$\sum_m^M \sum_n^N \left(S(m,n) - \bar{S}\right)^2$$

Here, G_x and G_y are the image gradients in the x and y direction respectively, computed using the Sobel gradient operators and $\overline{S}$ is the mean gradient in the gradient image S. Figure 4 shows the image of random cotton fibers acquired using WLCM, the image restored using LR algorithm at iteration 6 and the focus measures plotted at various LR iterations.

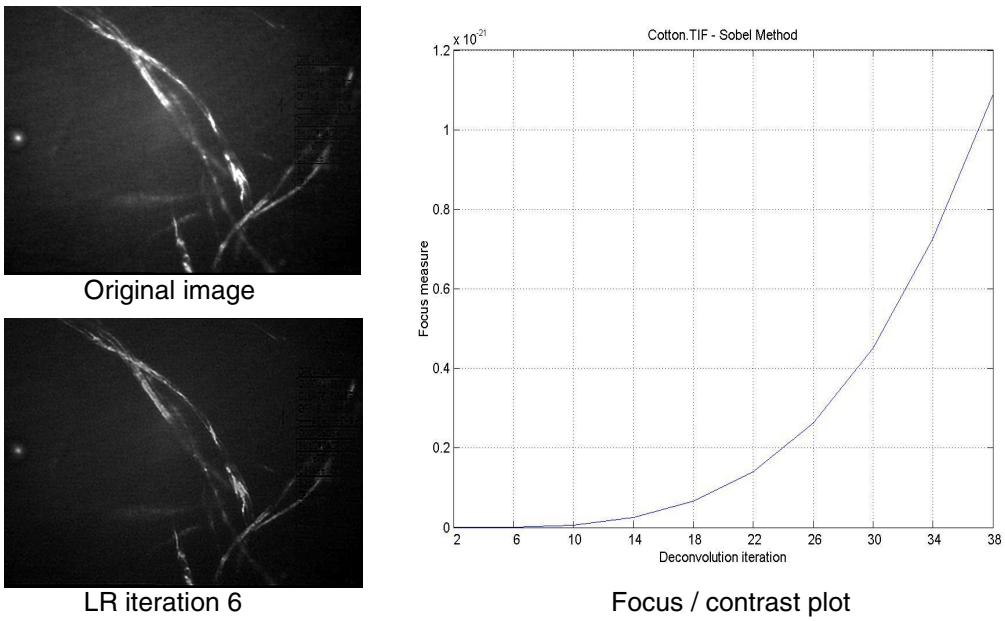

Figure 4. Images of a random cotton fiber restored using LR algorithm

An increasing trend in the focus measure plot confirms that the restoration algorithm reduces the blur. However we noticed that the focus measures did not converge due to the introduction of significant ringing artifacts at higher number of iterations. This led us to develop a ringing metric to quantify the amount of ringing artifacts introduced during iterative image restoration.

3.2. A ringing metric

The proposed ringing metric uses the edge profiles of the observed image g and the images restored f_k to isolate the ringing artifacts introduced during restoration. We create a reference edge profile E_{ref} of the unprocessed image g using canny edge detector. To detect the ringing artifacts in the restored images, we create a binary edge mask EM_{ref} by dilating the E_{ref} with a (r x r) structuring element where r is an approximate width in pixels from an edge to cover the ringing artifacts. We used an (8 x 8) structuring element. At the end of each iterative restoration step, we compute the edge profile E_n of the restored image. Now the edges and any ringing artifacts around the original edges can be selected by a simple pixel wise logical AND operation between EM_{ref} and E_n and stored in E_n(masked). Since restoration preserves the edges present in the reference image, the additional edges observed around the reference edge profile in the restored image typically represent the ringing artifacts. We define the following ringing metric to indicate the quality of the restored image.

$$\text{Ringing metric} = \left(\sum_i \sum_j E_n(masked) - \sum_i \sum_j E_{ref} \right) \Big/ \sum_i \sum_j E_{ref}$$

4. Results

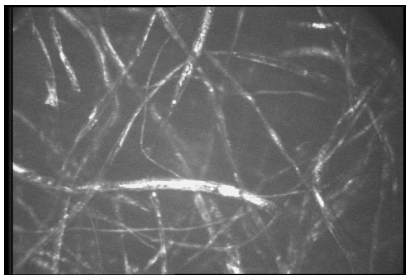

Unprocessed Image

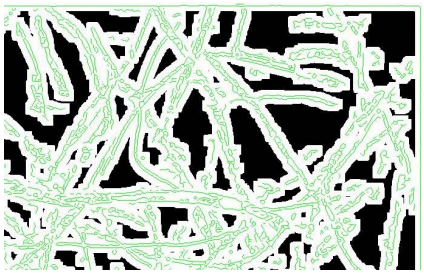

Reference edge profile (green) superimposed on binary edge mask (white background)

Figure 5. Unprocessed image *g* and its edge profile

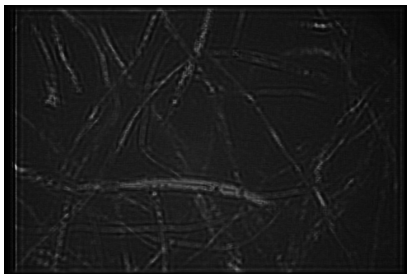

Restored image at iteration 10

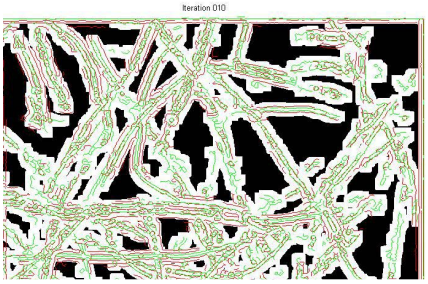

Restored-image's edge profile (Red) superimposed on binary edge mask (white background) and reference edge profile (green)

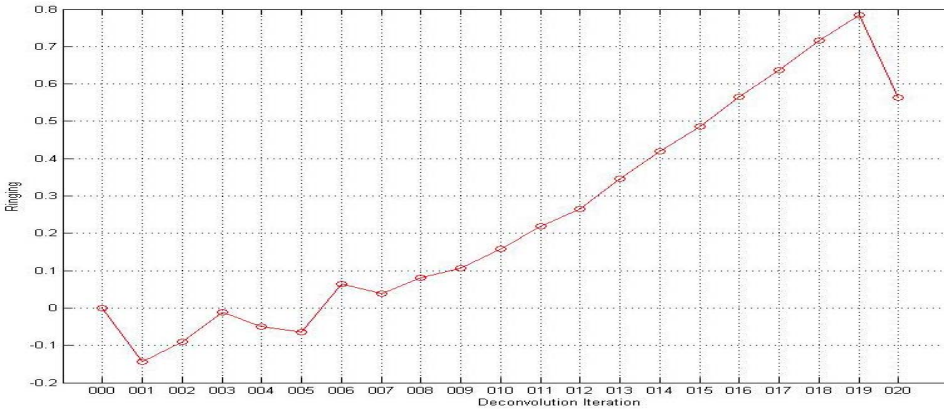

Ringing metric of the restored images at various LR iterative steps

Figure 6. Ringing metric of the images restored using LR iterative algorithm

Figure 5 shows the observed image and its edge profile E_{ref} superimposed on the binary edge mask. Figure 6 shows the image of a restored image exhibiting ringing artifacts, its edge profile superimposed on the reference edge profile and binary edge mask and the associated ringing metric plot obtained during LR iterative restoration. Increasing ringing-metric trend in the plot indicates the introduction of ringing artifacts at higher number of iterations and confirms with the visual inspection of the restored images.

5. Conclusion

Quantitative image analysis algorithms are sensitive to image artifacts. WLCM images are generally noisy and show a high degree of blur due to limitations of the optical system. Therefore, image restoration algorithms that utilize robust feedback metrics are necessary. The ringing metric proposed here is less sensitive to the noise amplification during restoration and is computationally efficient making it suitable for real-time image quality evaluation. Visual inspection of the restored images confirms the increase in ringing artifacts during restoration as pointed by the computed ringing metric. We are currently conducting a subjective experiment to evaluate the quality of the restored images in terms of the amount of ringing present. We will be using the proposed ringing metric for real-time restoration of WLCM images

6. Acknowledgement

This publication was made possible through a financial support in part from LA Board of Regents Health Excellence Fund HEF(2000-05)-01 and NIH grant number P20 RR16456. The contents presented in this publication are solely the responsibility of the authors and do not necessarily represent the official views of the funding agencies.

7. References

[1] J.B. Pawley, "Handbook of Biolofical Confocal Microscopy", Plenum press, 1995.
[2] http://www.olympusconfocal.com/theory, 2005.
[3] H.C. Andrews, B.R. Hunt, "Digital Image Restoration", Prentice-hall signal processing series, 1977.
[4] M.R. Banham, A.K. Katsaggelos, "Digital Image Restoration", IEEE signal processing magazine, pp. 24–41, March 1997.
[5] P.A. Jansson, "Deconvolution of images and spectra", Academic press, 2nd edition, 1997.
[6] J. Biemond, R.L. Lagendijk, R.M. Mersereau, "Iterative methods for Image Deblurring", Proceedings of the IEEE, Vol. 78, No. 5, pp. 856 -883, May 1990.
[7] D. Kundur, D. Hatzinakos, "Blind Image Deconvolution", IEEE signal processing magazine, pp. 43–63, 1996.
[8] EePing Ong, et.al., "A No-Reference Quality Metric for Measuring Image Blur", Seventh International Symposium on Signal Processing and Its Applications, 2003.
[9] Z. Wang, A.C. Bovik, "Why is Image Quality Assessment so Difficult?", IEEE International Conference on Acoustics, Speech & Signal Processing, May 2002.
[10] Z. Wang, A.C. Bovik, "A Universal Image Quality Index", IEEE Signal Processing Letters, Vol. 9, No.3, March 2002, pp.81-84.
[11] P. Marziliano, F. Dufaux, S. Winkler, T. Ebrahimi, "Perceptual Blur and Ringing Metrics: Application to JPEG2000", Sigman Processing: Image Communication, Vol. 19, No.2, Feb 2004, pp. 163–172.
[12] Yung-Kai Lai, "A Haar Wavelet Approach to Compressed Image Quality Measurement", Journal of Visual Communication and Image Representation, Vol. 11, 2000, pp. 17-40.
[13] Z. Wang, H.R. Sheikh, A.C. Bovik, "No-reference Perceptual Quality Assessment of JPEG compressed Images", Proceedings of International Conference on Image Processing, Vol. 1, 2002, pp. 477-480.
[14] K.R. Castleman, "Digital image processing", Prentice Hall, 1996.
[15] Y. Hiraoka, J.W. Sedat, D.A. Agard, "Determination of three-dimensional imaging properties of a light microscope system", Biophysical Journal, Vol. 57, pp. 325 – 333, February 1990.
[16] J.G. McNally, T. Karpova, J. Cooper, "Three-dimensional Imaging by Deconvolution Microscopy", Methods, Vol. 19, pp. 373 – 385, 1999.
[17] P.J. Shaw, D.J. Rawling, "The point-spread function of a confocal microscope: its measurement and use in deconvolution in 3-D data", Journal of Microscopy, Vol. 163, Pt 2, pp. 151 – 165, August 1991.
[18] S.F. Gibson, F. Lanni, "Experimental test of an analytical model of aberration in an oil-immersion objective lens used in three-dimensional light microscopy", Journal of. Optical Society. of America A, Vol. 8, No. 10, pp. 1601 – 1613, October 1991.
[19] Rafael C. Gonzalez, Richard E. Woods, "Digital Image Processing", Prentice-hall, 2nd Edition, January 2002.
[20] J.L. Pech-Pacheco. G. Cristobal, J.C. Martinez, J.F. Valdivia, "Diatom autofocusing in brightfield microscopy: a comparative study", 15th International Conference on Pattern Recognition, 2000, pp. 314-317.